Research on amultiscale approach to tubular structure detection in 3D biomedical images

Shihai Zhu*
College of Information Engineering and Art Design,
Zhejiang University of Water Resources and Electric Power, Hangzhou 310018,
(P.R.CHINA)
E-mail: yyzz98@163.com

ABSTRACT

Image detection is an important technology which has been applied extensively to geometric measurement, industrial quality inspection, three-dimensional surface detection and the like. Because most of image detection algorithms are effective for specific problems so far, there is no detection algorithm can be applied to solve all image detection problems. Detection of tubular structures in 3D medical images is an important issue for vascular medical imaging. In this paper, we propose a new adaptive medialness measure for detection of tubular structures in 3D medical images. The adaptiveness of the medialness is based on the Hessian matrix of the image, its eigenvectors and eigenvalues. First we describe the proposed measure of medialness and ridge, Second we use a simple model of cylindrical vessel with circular Gaussian cross-section to illustrate our detection solution, meanwhile we give the relationship between the size of the structure and its selected scales. From this relationship, we explain the extraction of local extrema and make a full reconstruction of the vessels network. Thirdly synthetic and real images are used to verify our study under the suggested tubular structures. At last we draw some conclusions and give some areas for future research.

KEYWORDS

Vessel structure; Multiscale response; 3D biomedical imaging; Synthetic image; Vessel network reconstruction.

INTRODUCTION

Detection of tubular structures in 3D images is an important issue for vascular medical imaging. In[1], Koller et al. propose a multiscale response in order to detect linear structures in 2D images, the response function uses eigenvectors of the Hessian matrix of the image. After that, in[2], Lorenz et al. decided to use further information from the Hessian matrix, that is, its eigenvalues. A more recent work done by Sato et al. in[3-8], they also propose to choose a response function based exclusively on the eigenvalues of the Hessian matrix. The choice of the response function which combines the three eigenvalues is heuristic. Their approach is to provide a visual help in the interpretation of the image after filtering. However, the images used in their experiments seem to have a higher spatial resolution than usual images used in clinical practice, and their algorithm doesn't detect vessel axes and doesn't seem suitable for an accurate estimation of vessel size. In[9-12], Frangi et al. propose another response function by interpreting geometrically the eigenvalues of the Hessian matrix.

In this paper, we present a new approach for detection of tubular structures in 3D images. A way to take into account the varying size of vessels in the image is to apply a multiscale analysis that allows us to detect structures of various sizes according to the scale at which they give a maximal response. then we extract the local extrema in this multiscale response in order to estimate the vessels centerlines. Afterwards vessels are reconstructed using both the centerlines and the size information. Finally synthetic and real images are used to show the behavior of the algorithm under the suggested tubular structures.

BASIC CONCEPTS AND THE SUGGESTED MODEL

Linear scale space

When applying the approach of multiscale analysis to an image, the use of the convolution product with a Gaussian kernel has been shown to be the only way to ensure the following properties: linearity, invariance under translation, invariance under rotation and invariance under rescaling[13-15]. Florack and et al.[16] show that the evolution through scales can be written using two dimensionless variables L/L_0 and x/σ. σ denotes the standard deviation of the Gaussian kernel, L_0 is the response obtained from the initial image and L is the response obtained at a scale $t = \sigma^2$. In this paper[14], Lindeberg shows the necessity of normalizing the derivatives of the image in the multiscale analysis. He introduces the notion of γ-normalized derivatives:

$$\partial_{x,\gamma-norm} = t^{\gamma}\partial_x \tag{1}$$

When the parameter γ equals one, the normalization ensures invariance under image rescaling, which is compatible with the dimensionless variable $u = x/\sigma$:

$$\frac{\partial I}{\partial u} = \frac{\partial I}{\partial x}\frac{\partial x}{\partial u} = \sigma\frac{\partial I}{\partial x} \tag{2}$$

Medialness and ridge

In[17], Eberly and et al. reviewed the different definitions of ridges and their invariance properties. They also proposed an extension of the concept of ridges of dimension d in n-dimensional images, which is listed below.

If $I(\overline{x})$ is a real-valued function defined for $\overline{x} \in R^n$, and $H(\overline{x})$ is the Hessian matrix of I at $\overline{x}$. Assuming that the eigenvalues of $H(\overline{x})$ are ordered as $\lambda_1 \leq \cdots \leq \lambda_n$ with associated eigenvectors $(v_i)_{i\in[1,n]}$, and $\overline{x}$ is a ridge point of type n-d if and only if $[v_1 \cdots v_d]^t \nabla I(\overline{x}) = 0$ and $\lambda_d < 0$ with $1 \leq d \leq n$.

In[18-21], the medialness was defined as a convolution product of the initial image with a kernel $K(x,\sigma)$, that is, $M(x,\sigma) = I(x) * K(x,\sigma)$.

Suggested model: cylindrical circular model with gaussian cross-section

The suggested vessel model is cylindrical where(Oz)is the vessel axis and the vessel section is a Gaussian blob. In this section, we use the following notations:

-I_0 is the initial image,

-σ_0 denotes the radius of the initial vessel model which is also the standard deviation of a Gaussian,

-G_{σ} is a Gaussian function with standard deviation σ ,

-H is the Hessian Matrix of the image, H' is a simplified matrix proportional to H,

-λ_1, λ_2, λ_3 are eigenvalues of the Hessian matrix with $|\lambda_1| \geq |\lambda_2| \geq |\lambda_3|$,

- $\vec{v_1}, \vec{v_2}, \vec{v_3}$ are the associated eigenvectors.

Therefore in this model, there is

$$I_0(x, y, z) = CG_{\sigma 0}(x, y) = \frac{C}{2\pi\sigma_0^2} e^{-\frac{x^2+y^2}{2\sigma_0^2}} \tag{3}$$

Where C is a function of σ_0 and $\frac{C}{2\pi\sigma_0^2}$ represents the intensity at the center of the vessel,described as Figure 1. C depends on the size of the vessel, this dependence is due to partial volume effect that decreases the small vessels' intensity.
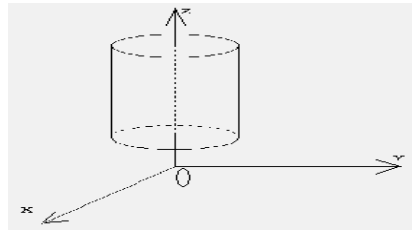

Figure 1 : Suggested model of a vessel

ALGORITHM OF TUBULAR STRUCTURE DETECTION

Our algorithm can be split into a few steps. First we compute the multiscale response from responses at a discrete set of scales, Then we extract the local maxima in this multiscale response in order to estimate the vessels centerlines. In the following vessels are reconstructed using both the centerlines and the size information. In the first step, we use a model of the vessels both for interpreting the eigenvalues and the eigenvectors of the Hessian matrix and for choosing a good normalization parameter.

Some notations frequently used in this paper are listed in TABLE 1.

TABLE 1 : Some notations frequently used in this paper

Notation	Meaning
t	the current scale
$M(\bar{x})$	point in the definition domain of the image I_0, $\bar{x} = (x, y, z) \in R^3$
$R_t(\bar{x})$	the response for a scale t and at a given location $\bar{x}$
R_t^n	thenormalized response for a scale t
γ	normalized parameter
t_{max}	the scale at which thenormalizedresponse is maximal
$L(\bar{x}, t) = I_0(\bar{x}) * G_{\sqrt{t}}(\bar{x})$	the image at a scale t
G_σ	Gaussian function with standard deviation σ

Computation of the response R_t at one scale t

For a point $\bar{x}$, the response is set to the minimum of the absolute value of theintensity's first order derivative computed at 4 points equidistant from $\bar{x}$. An advantageof this choice is to ensure that a high response results in a high probability of being at avessel's center, but this medialness response is too sensitive to noise. It seems more naturalto use information from the first derivative at every point of a circle than just four points. This circle $C(\bar{x}, \theta\sqrt{t})$ iscentered at the current point $\bar{x}$, has a radius $\theta\sqrt{t}$ and is in the planedefined by $\bar{x}$ and the two eigenvectors $\vec{v_1}$ and $\vec{v_2}$. The proportionality constant θ will bechosen according to the model. This constant is the inverse of the constant $\rho = \frac{1}{\theta}$ alreadyintroduced in[14,15].

Under this condition, we propose to use the following medialness response

$$R_t(\bar{x}) = \frac{1}{2\pi} \int_0^{2\pi} -\nabla_t I_0(\bar{x} + \theta\sqrt{t}\vec{v_\alpha}) \cdot \vec{v_\alpha} d\alpha \tag{4}$$

With $\vec{v_\alpha} = \cos(\alpha)\vec{v_1} + \sin(\alpha)\vec{v_2}$.

This response is the mean of first order derivative information taken at the circle $C(\bar{x}, \theta\sqrt{t})$. $\vec{v_\alpha}$ is the radial direction and $\nabla_t I_0$ is the gradient vector of the initial image, computed at the scale t.

Computation of multiscale responses

One difficulty with multiscale approach is that we want to compare the result of a response function at different scales while the intensity and its derivatives are decreasing functions of scale. Lindeberg[14]introduced the notion of normalized derivatives in order to deal with this problem. If the scale t is defined as $t = \sigma^2$ where σ is the standard deviation of the Gaussian, the γ-normalized derivative ∂_γ was already defined by equation 1.

At a scale t, the cylindrical circular model with a constant C>0 leads to

$$L(\bar{x}, t) = I_0(\bar{x}) * G_{\sqrt{t}}(\bar{x}) = CG_{\sqrt{\sigma_0^2 + t}}(\bar{x}) \cdot \tag{5}$$

The calculation process of the maximum of the normalized response R_t^n is listed below.

We aim to detect the axis of the vessel which is defined by x=y=0, the response at a point M(0,0,z)is given:

$$R_t(\bar{x}) = \frac{1}{2\pi\theta\sqrt{t}} \int_0^{\theta\sqrt{t}} \left| \nabla L(\bar{x}, t) \cdot \vec{n} \right| d\bar{x} \cdot \tag{6}$$

The gradient and the normal vector $\vec{n}$ are formulated as

$$\nabla L(\vec{x}, t) = L(\vec{x}, t) \frac{-1}{t + \sigma_0^2} \begin{pmatrix} x \\ y \\ 0 \end{pmatrix}, \vec{n} = \frac{1}{\sqrt{x^2 + y^2}} \begin{pmatrix} x \\ y \\ 0 \end{pmatrix}$$

with $x^2 + y^2 = \theta^2 t$. Therefore,

$$\left| \nabla L(\bar{x}, t) \cdot \vec{n} \right| = C \frac{\theta\sqrt{t}}{2\pi(t + \sigma_0^2)^2} e^{-\frac{\theta^2 t}{2(t + \sigma_0^2)}} \cdot \tag{7}$$

The last expression is no longer a function of $\bar{x}$, then the mean of this expression along the circle is straightforward, and

$$R_t = C \frac{\theta\sqrt{t}}{2\pi(t + \sigma_0^2)^2} e^{-\frac{\theta^2 t}{2(t + \sigma_0^2)}} \cdot \tag{8}$$

The normalized response R_t^n is defined by $R_t^n = t^{\gamma/2} R_t$, and its partial derivative on t is:

$$\frac{\partial R_t^n}{\partial t} = A \frac{Ct^{\gamma - 1/2}}{4\pi(t + \sigma_0^2)^4} e^{-\frac{\theta^2 t}{2(t + \sigma_0^2)}}, \tag{9}$$

With $A = (\gamma - 3)t^2 + (2\gamma - 2 - \theta^2)\sigma_0^2 t + (1 + \gamma)\sigma_0^4$.

We are looking for the value of γ which gives a maximum for the function R_t^n at $t = \sigma_0^2$. Thus we want $\frac{\partial R_t^n}{\partial t}$ to have a positive root which corresponds to a maximum.

The sign of $\frac{\partial R_t^n}{\partial t}$ is the same as the sign of A, when $\gamma < 3$ and the determinant Δ is also positive, has onlyone positive root which corresponds to a maximum for R_t^n

$$R_t^n = C \frac{\theta t^{\frac{\gamma + 1}{2}}}{2\pi(t + \sigma_0^2)^2} e^{-\frac{\theta^2 t}{2(t + \sigma_0^2)}} \tag{10}$$

We find a a relation of proportionality between the scale t_{max} that gives a maximal response and the initial radius of the vessel σ_0 :

$$t_{max} = h(\gamma, \theta)\sigma_0^2 \tag{11}$$

Where h is a function of the normalization parameter γ and the proportionality constant θ :

$$h(\gamma, \theta) = \frac{\sqrt{\Delta} - 2\gamma + 2 - \theta^2}{2(3 - \gamma)} \tag{12}$$

With $\Delta = [\theta^2 - (2\gamma - 2)]^2 + 16 - (2\gamma - 2)^2$. Usually, γ is chosen to allow the response R_t to be maximal for a scale corresponding to the size of the structure we want to detect. To keep generality, we establish the relationship between the scale t_{max} where the maximal response is reached and the initial radius σ_0 of the vessel. This relationship depends on both the normalization parameter γ and the distance coefficient θ.

Once we have chosen the two parameters γ and θ, we can deduce two numerical relations for our model. That is, $t_{max} = h(\gamma, \theta)\sigma_0^2 = 0.5\sigma_0^2$,

$$R_{t_{max}}^n = [\frac{C}{2\pi\sigma_0^2}]\sigma_0^{\gamma-1} \frac{\theta h(\gamma, \theta)^{\frac{\gamma+1}{2}}}{(h(\gamma, \theta) + 1)^2} e^{-\frac{\theta^2 h(\gamma)}{2(h(\gamma)+1)}} \tag{13}$$
$$\approx 0.232 [\frac{C}{2\pi\sigma_0^2}]$$

This value is proportional to the intensity of the vessel center when the background intensityis null. $R_{t_{max}}^n$ is approximately equal to 0.232 times the intensity at the vessel center $\frac{C}{2\pi\sigma_0^2}$.

Reconstruction and visualization

It is not an easy task to visualize the local extrema image in order to improve the interpretation of the original data image. For that purpose, we propose to extract some information from the local extrema image, to superimpose it into some 3D representation of the original data image or to use it for a vessel network reconstruction. It can be described in detail as below.

1) Line extraction

In order to obtain the centerlines from the local maxima image, we first binarize the local extrema image by applying a hysteresis thresholding. Second, we thin this result to obtain a skeleton-like representation of the vessels. The resulting skeleton is composed of pieces of curves, each of them representing a piece of vessel. Third, the skeleton is simplified by removing small pieces of curves. The result obtained is an image of the vessel axes.

2) Reconstruction

The centerline image also contains information about the size of the vessel, which is proportional to the scale at which the current point has been extracted.

3) Visualization

In both cases, MIP view or isosurface, the superimposition of the detected 3D centerlines can help the interpretation of the real vessel network. Moreover, an isosurface of the reconstructed vessel network has the advantages of an initial image isosurface without having its drawbacks, because all vessels are reconstructed with the same centerline intensity. Thus, it can help to understand the local structure of the vessels network.

EXPERIMENTS AND RESULTS

In this section, we present some experiments made on synthetic images and real images.

Experiments on synthetic images

The created images have a Gaussian blob cross-section and their difference from the theoretical models lies in their discrete representation.
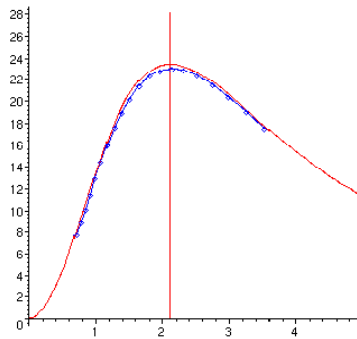
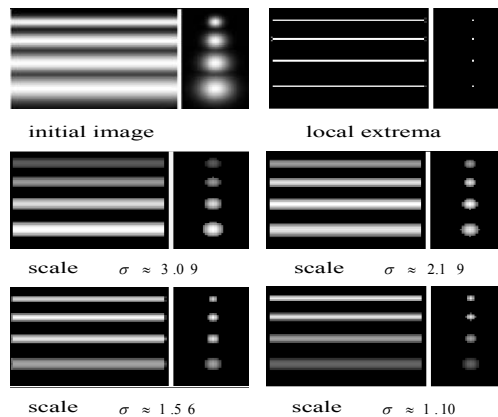**Figure 2 : Response obtained at the center of the vessel for different scales**

Figure 3 : Responses obtained for the optimal scales

As mentioned above, we made some experiments on cylindrical circular vessels with Gaussian cross-section.

(1)Response profile

The response profile is the evolution of the medialness response as a function of scale, here taken at the vessel center. Figure 2 shows a comparison between thetheoretical and the obtained profiles. In red, the theoretical profile, and in blue, the obtained profile. The vertical red line shows the theoretical scale for which the response is maximal The synthetic image contains a circular cylinder with Gaussian blob cross-section, radius 3 voxels and intensity equal to 100 at the center. The theoretical response profile is given by equation 10where $\sigma_0 = 3$, $\gamma = 1$, $\theta = \sqrt{3}$ and $C = 2\pi\sigma_0^2 \times 100$. The experimental response profile is obtained from twenty scales ranging from 0.7 to 8. This comparison shows that the two profiles match, and that the experimental profile is slightly lower than the theoretical one near the maximal scale.

(2)Normalization

The relationship between the vessel radius and the optimal scale is $t_{max} = h(\gamma, \theta)\sigma_0^2 = 0.5s_0^2$ where s_0 is the radius of the vessel with Gaussian-like cross-section. The response at the optimal scale and at thevessel center should be equal to $R_{t_{max}}^n$ times the intensity at the vessel center, described as in equation 13. The initial image of Figure 3 contains four vessels with Gaussian blob cross-section and respective radii are 1.25,1.75,2.5,8.

We applied the multiscale analysis on this image with 20 scales for vessels radiiranging from 1 to 4 voxels. The difference between the obtained maximal responseand the theoretical expected value is stronger for small vessels and is probably due tothe trilinear interpolation of the gradient vector during the response computation. Thisdifference remains small, below 11%, which confirms the zoom invariant property of thenormalization, and will allow an easy threshold of the local extrema image, as shown in Figure3.

Experiments on real images

(1)Image acquisition

Our algorithm was tested on a set of images, which are obtained by 3D reconstruction of the vessels from 2D X-ray substracted angiographies. Details of the reconstruction scheme can be found in[11]. Compared to the other 3D acquisition

modalities which are Magnetic Resonance Angiography and Scanner Angiography, this 3D reconstruction gives a high isotropic resolution over the whole reconstructed volume. However, it requires a good opacification of the vascular network obtained with an intra-arterial injection. The left images in Figure 4 are MIP views of a typical sub-images centered on an aneurysm. They contain different artefacts: noise, partial volume effect, consequences of the patient motion between different acquisitions and 3D reconstruction artefacts which lead to a non-homogeneity of the intensity of the vessels for different sizes of the vessel. The two right columns of Figure 4 show isosurfaces of the images, where small vessels are only visible with a low threshold (surface holes in black are due to the image boundaries).

(2) Choice of parameters

We tested our algorithm on ten images 128×128×128 of varying complexity. Because small vessels have a lower intensity than bigger ones, we used a parameterγlower than 1 for the normalization. Decreasing the value of γ has the effect of enhancing small vessels compared to big ones, and helps to compensate for intensity variations. We used the value 0.75 for γ. The minimum and maximum scales are chosen according to the radii of the thinnest and the thickest vessels in the initial image. The algorithm was run with scales that detect vessels of radii ranging from 0.4 to 6 voxels. Then, after manual thresholding, the centerlines extraction takes a few seconds.

(3) Results

Results on the three images of Figure 4 are shown in Figure 5. On the left, the detected centerlines are represented with an isosurface of the initial image and using transparency. On the right, a surface of the reconstructed network is represented, the reconstruction is based on the previous centerlines and the estimated radii. In Figure 6, on the left, detected centerlines are superimposed on an isosurface of the initial image. On the right, reconstruction of the vessels network is made from centerlines and radii estimation.
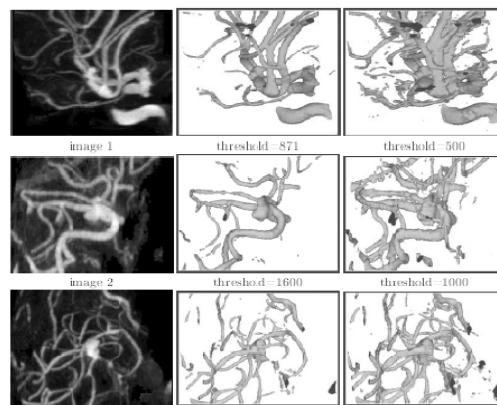

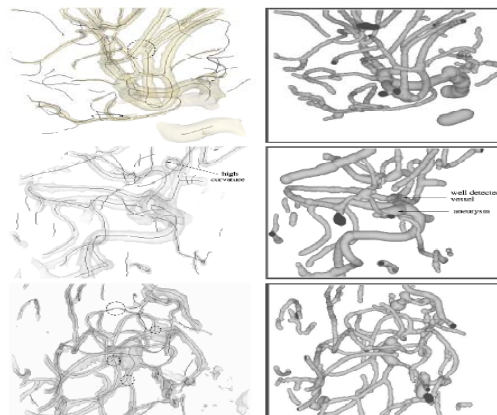**Figure 4 : Top, MIP view and isosurfaces of three X-ray 3D images**

Figure 5 : Results on the images represented in figure 4

CONCLUSIONS AND FUTURE WORK

We presented a multiscale approach for tubular structures detection in 3D medical images. Our approach used gradient information at a given distance of the vessels centers. Using a cylindrical circular model with Gaussian blob cross-

section, we found the optimal distance for computing gradient information at a given scale, and we also expressed the vessel radius as a function of the maximal scale.

Next, we proposed an algorithm for extracting centerlines and reconstructing the whole vessels network. Experiments on synthetic and real images show the results of the approach according to radius variations for vessels with Gaussian cross-sections.

There are a number of areas for future research that couldclarify and extend the results of the present study. First, it is important to extractthe vessels centerlines in order to ensure their continuity to understand the topology of the vessels network. Second, it is an important issue to discriminate between vessel and non-vessel structures. This discrimination is present in ouralgorithm at the pre-selection stage based on Hessian matrix eigenvalues and also in the response function that enhances vessel centers. However, another discrimination of the local maxima may be necessary when the image contains non-vessel structures with high gradients or to remove wrongextrema obtained near the vessels frontiers. Finally, once a good detection of the centerlines is obtained, a second andmore precise detection of the vessels contours may be done based on this information and without assuming a circular cross-section profile.

ACKNOWLEDGEMENTS

REFERENCES

[1] T.M.Koller, G.Gerig, G.Szekely, D.Dettwiler; "Multiscale detection of curvilinear structures in 2D and 3D images data", IEEE ICCV', 864-869 **(1995)**.

[2] C.Lorenz, I.C.Carsen, T.M.Buzug, C.Fassnacht, J.Weese; "Multiscale line segmentation with automatic estimation of width,contrast and tangential direction in 2d and 3d medical images", CVRMed-MRCAS', 213-222 **(1997)**.

[3] Y.Sato, S.Nakajima, N.Shiraga, H.atsumi et al.; "Three-dimensional multiscale line filter for segmentation and visualization of curvilinear structures in medical images", Journal of Medical Image Analysis, **12**, 143-168 **(2008)**.

[4] Y.T.Kao, H.J.Lin, C.W.Wang, Y.C.Pai; "Effective detection for linear up-sampling by a factor of fraction", IEEE Trans.Image Process., **21(8)**, 3443–3453 **(2012)**.

[5] T.Brox, J.Weickert; "Level set segmentation with multiple regions", IEEE Trans.Image Process, **(15)**, 3213–3218 **(2006)**.

[6] D.Joshi, N.Londhe; "Automatic liver tumour detection in abdominal ct images", Int.J.Comput.Technol.Electron.Eng., **3**, 25–30 **(2013)**.

[7] Jian-Lei Liu, Da-Zheng Feng; "Two-dimensional multi-pixel anisotropic Gaussian filter for edge-line segment (ELS) detection", Image and Vision Computing, **32**, 37–53 **(2014)**.

[8] Jianfei Liu, Shijun Wang, Marius George Linguraru, Jianhua Yao, Ronald M.Summers; "Tumor sensitive matching flow: A variational method to detecting and segmenting perihepatic and perisplenic ovarian cancer metastases on contrast-enhanced abdominal CT", Medical Image Analysis, **18**, 725–739 **(2014)**.

[9] F.Frangi, A.Colchester, S.Delp; "Multiscale vessel enhancement filtering",MICCAI', 130-137 **(2011)**.

[10] H.Abdelmunim, A.Farag, A.A.Farag; "Shape representation and registration in vector implicit spaces: Adopting a closed form solution in the optimization process", IEEE Trans.Pattern Anal.Mach.Intell., **35(3)**, 763–768 **(2013)**.

[11] A.Ali, A.Farag, A.Farag; "Multimodal imaging: Modeling and segmentation with biomedical applications," IET Comput.Vis., **6(6)**, 524–539 **(2012)**.

[12] Chenglong Chen, Jiangqun Ni, Jiwu Huang; "Blind detection of median filtering in digital images: A difference domain based approach", IEEE Transactions on Image Processing, **22(12)**, 4699-4710 **(2013)**.

[13] T.Lindeberg; "Scale-space theory in computer vision", Kluwer academic publishers, Dordrecht, Netherlands, **(2004)**.

[14] T.Lindeberg; "Edge detection and ridge detection with automatic scale selection", IEEE CVPR', 465-475 **(2006)**.

[15] Zhiwei Ye; "Image segmentation using thresholding and swarm intelligence", Journal of software, **7**, 1074-1082 **(2012)**.

[16] L.M.Florack, B.M.Ter Haar Romeny, J.J.Koenderink, M.A.Viergever; "Scale and the differential structure of images", Journal of Image and Vision Computing, **30**, 376-388 **(2012)**.

[17] D.Eberly, R.Gardner, B.Morse,S.Pizer, C.Scharlach; "Ridges for image analysis", Journal of Mathematical Imaging and Vision, **4**, 353-373 **(2004)**.

[18] S.M.Pizer, D.Eberly, D.Fritsch, B.S.Morse; "Zoom-invariant vision of figural shape", Journal of Computer Vision and Image Understanding, **69**, 55-71 **(2008)**.

[19] Cunliang Liu; "SAR image segmentation based on fuzzy region competition algorithm and gamma model", Journal of software, **8**, 228-235 **(2013)**.

[20] Amal A.Farag, Hossam E.Abd El Munim, James H.Graham, Aly A.Farag; "A novel approach for lung nodules segmentation in chest CT using level sets", IEEE Transactions on Image Processing, **22(12)**, 5202-5213 **(2013)**.

[21] A.C.Jirapatnakul, Y.D.Mulman, A.P.Reeves, D.F.Yankelevitz, C.I.Henschke; "Segmentation of juxtapleural pulmonary nodules using a robust surface estimate," Int.J.Biomed.Imaging, **2011**, 1–14, **(2011)**.